NF1 loss as a driver of bone metastasis in estrogen receptor-positive breast cancer

Zhao, Zifan[1,2]; Zheng, Ze-Yi[1,3]; Lei, Jonathan T.[1,5]; Baik, Matthew J.[1]; Wu, Yi-Hsuan[1,2]; Somes, Lauren K.[1,2]; Harb, Omar A.[1]; Wang, Junkai[1]; Rasaily, Uttam[4]; Chang, Owen A.[6]; Wang, Hai[1,4]; Bado, Igor[1,4]; Gugala, Zbigniew[7]; Anurag, Meenakshi[1,3]; Zhang, Bing[1,5]; Sreekumar, Arun[4]; Hoyos, Valentina[1]; Zhang, Xiang H.-F.[1,4], Chang, Eric C.[1,4]

[1]Lester and Sue Smith Breast Center, [2]Cancer & Cell Biology Graduate Program, Department of [3]Medicine, [4]Molecular and Cellular Biology, [5]Molecular and Human Genetics, Baylor College of Medicine, USA.
[6]DeBakey High School for Health Professional. [7]Department of Orthopedic Surgery and Rehabilitation, University of Texas Medical Branch

Abstract

Approximately 80% of breast cancers (BCa) expresses estrogen receptor-α (ER), and ER$^+$ BCa most frequently metastasizes to the bone. The driver of bone metastasis remains undefined. To address this unmet need, we focus on a key tumor suppressor, neurofibromin (NF1), which is both a GTPase-activating protein that represses RAS signaling and a direct transcriptional corepressor that represses ER.

In a clinical cohort of patients who later developed metastases, we found NF1 copy-number loss (CNL) in 62% of ER$^+$ tumors and enriched specifically in bone metastases. Using mammary fat pad injection followed by primary tumor resection, luciferase-tagged NF1-knockout (NF1^{KO}) ER$^+$ BCa cells exhibited markedly increased dissemination to bone compared with NF1$^+$ controls. Intra-iliac artery injection further demonstrated accelerated NF1^{KO} cell growth within the bone microenvironment.

Because ER$^+$ bone metastasis is driven in part by osteoclast (OC) formation, we examined the impact of NF1 loss on cancer-bone cell interactions. In co-culture assays, NF1-depleted ER$^+$ BCa cells enhanced RANKL-induced OC differentiation, accompanied by elevated expression and secretion of ICAM1, a key mediator of OC precursor fusion. Pharmacological ICAM1 inhibition attenuated this effect. Additionally, NF1^{KO} BCa cells suppressed proliferation and IFNγ production in primary human T cells and were more resistant to HER2-targeting CAR-T cytotoxicity while inducing CAR-T apoptosis.

Collectively, these findings support a model in which NF1 loss simultaneously promotes osteoclastogenesis and immune suppression, thereby enabling ER$^+$ BCa progression in bone. Targeting NF1-regulated RAS and ER pathways may provide new therapeutic strategies to mitigate bone metastasis in NF1-deficient ER$^+$ breast cancer.

Results

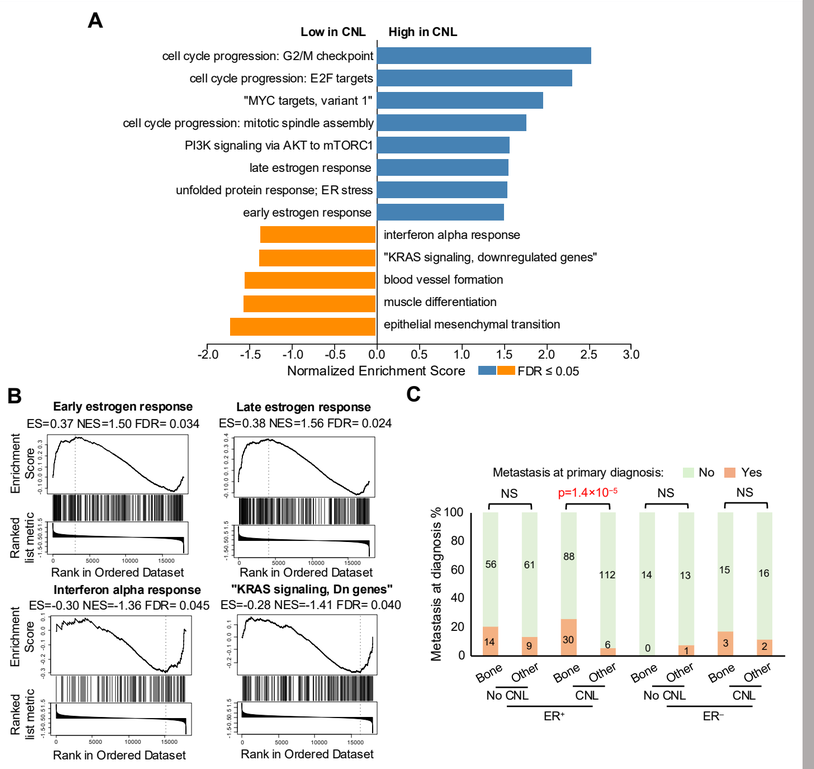
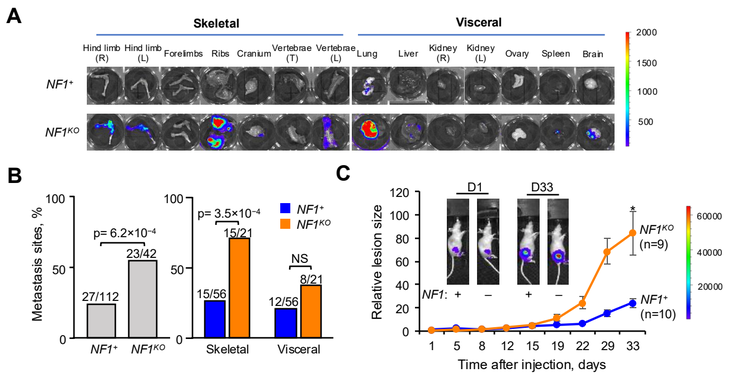


Fig. 1. *NF1* copy number loss (CNL) is common in ER$^+$ bone metastases (**A**) Hallmark pathway enrichment analysis comparing ER$^+$ samples with vs without *NF1* CNL. (**B**) GSEA leading edge analysis on *Estrogen response early, Estrogen response late, KRAS signaling downregulated* and *Interferon alpha response* pathways. (**C**) Bar graph showing number of cases, stratified by the status of *NF1* CNL and ER, presented with metastases at the time of primary diagnosis in bone vs. other tissues. P-values by Pearson's χ^2-test. NS, not significant.



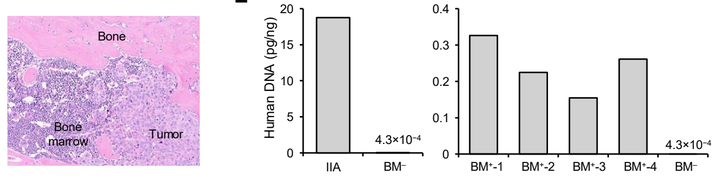


Fig. 2. Efficient dissemination to and growth in the bone by NF1-depleted ER$^+$ breast cancer cells. (**A**) Luc-labeled *NF1*$^+$ or *NF1*^{KO} MCF7 cells were injected into the mammary fat pad of NSG mice, and the primary tumors were removed when reached 1 cm in diameter. *Ex vivo* imaging was performed on seven skeletal and seven visceral organs per mice 40 days post-surgery. Metastasis positivity was determined based on IVIS signal. (**B**) Bar graph showing percentage of metastasis by sites. P-value by Pearson's χ^2-test. NS, not significant. (**C**) The growth of luc-labeled *NF1*$^+$ or *NF1*^{KO} MCF7 cells in hind leg after intra-iliac artery (IIA) injection (7) was measured by IVIS imaging. P-value was calculated using Student's t-test. *P<0.05. (**D**) H&E staining of an IIA femur sample. (**E**) Human DNA level in mouse tissues measured by Femto human DNA quantification kit. BM, bone metastasis.

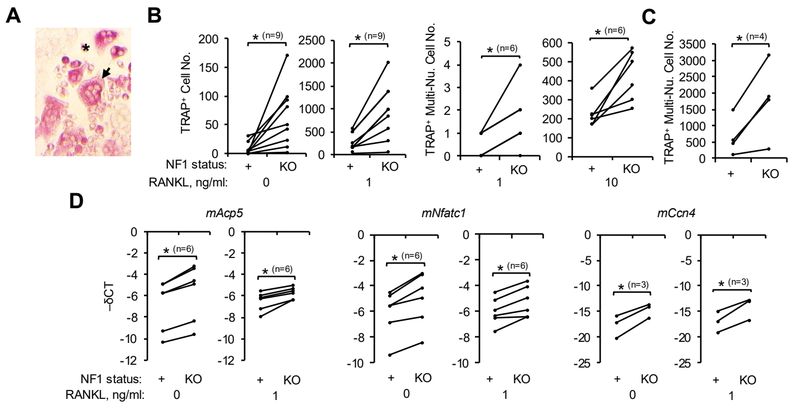


Fig. 3. NF1-depleted ER$^+$ breast cancer cells promote OC formation in co-culture with OC progenitor cells. (**A**) *NF1*$^+$ or *NF1*^{KO} MCF7 cells were cocultured with a mouse OC progenitor cell line, RAW264.7 cells, in the presence of 1 or 10 ng/ml RANKL. After 6 days, the cells were fixed and stained for TRAP activity, which marks the cells red. Asterisk, single nucleated TRAP$^+$ cell. Triangle, double nucleated TRAP$^+$ cell. Arrow, multi-nucleated TRAP$^+$ cell. (**B**) Quantification of TRAP$^+$ multinucleated cells. (**C**) Quantification in primarily cultured human monocytes. (**D**) RT-qPCR of OC marker genes: *mAcp5, mNfatc1* and *mCcn4*. The results are stratified by the *NF1* status of MCF7 cells and RANKL concentration. Similar results were observed with T47D cells. P-values were calculated by paired t-tests. *P<0.05.

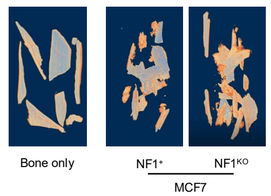
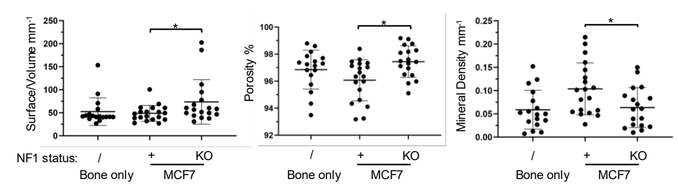


Fig. 4. NF1-depleted ER$^+$ breast cancer cells induce bone resorption *in vitro*. (**A**) *NF1*$^+$ or *NF1*^{KO} MCF7 cells were co-cultured with bone fragments taken from mouse hind leg for 5 weeks. Bone structural changes were measured using μCT scanning. Tumor-free bones were scanned as a control. Orange color represent bone erosion. (**B**) Quantification of surface-to-volume ratio and porosity. P-values were calculated by t-test. *P<0.05.



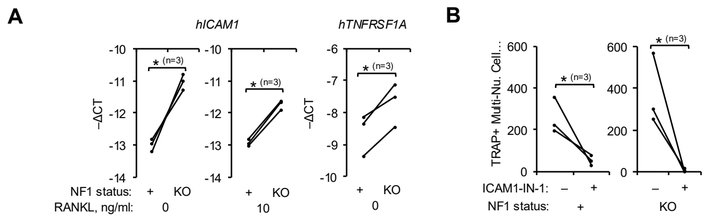


Fig. 5. ICAM1 induced in NF1-depleted breast cancer cells is required for OC formation. (**A**) MCF7 and RAW264.7 cells were co-cultured as in Fig. 3. Expression of human *ICAM1* (*hICAM1*) and *TNFRSF1A* (*hTNFRSF1A*) stratified by NF1 status of cancer cells and RANKL treatment was analyzed by qPCR. (**B**) OC formation as measured by TRAP assay in the presence of an ICAM1 inhibitor, ICAM1-IN-1. P-values by paired t-tests. *P<0.05.

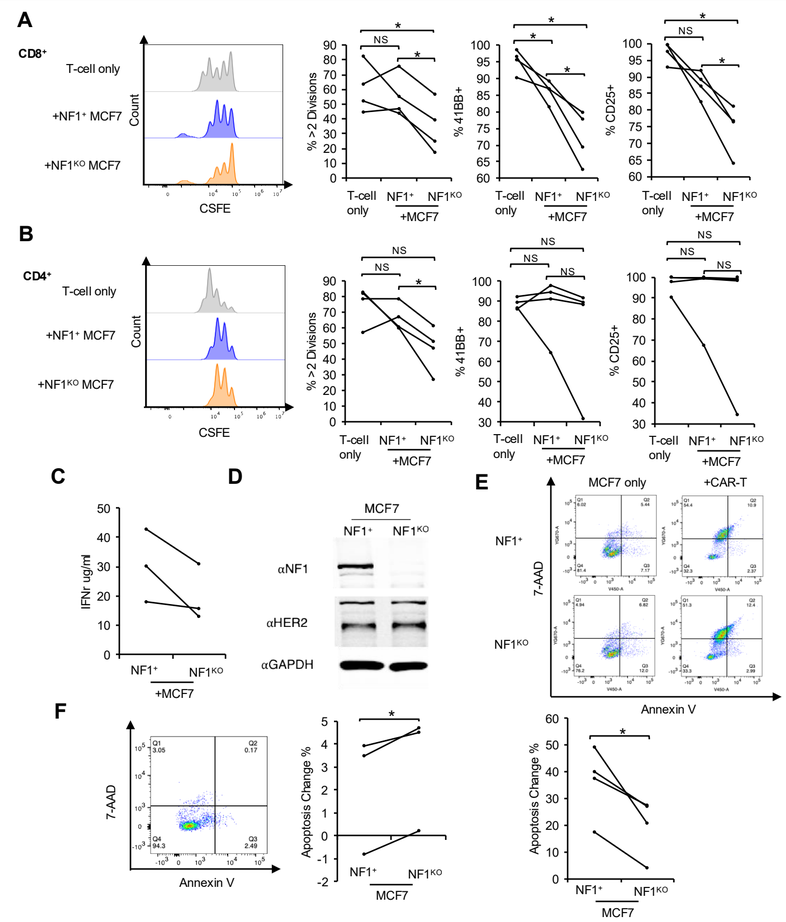
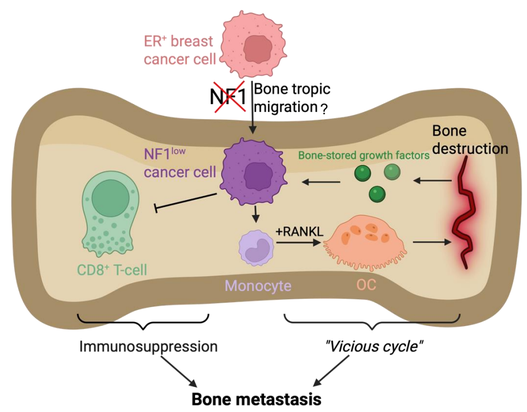


Fig. 6. NF1-depleted ER$^+$ breast cancer cells selectively suppress CD8$^+$, but not CD4$^+$, T-cell activity (**A**) T-cells were isolated from human PBMCs using the anti-CD3 microbeads and labeled by CFSE (5,6-carboxyfluorescein diacetate succinimidyl ester. T-cell proliferation was stimulated by anti-CD3/CD38 mAb and IL-2. After 72 hours incubation with *NF1*$^+$ or *NF1*^{KO} MCF7 cells, T cells were labeled by CD3-APC AF750, CD4-Krome Orange, CD8-PerCP, 41BB-PE, and CD25-APC. CD8$^+$ (**A**) and CD4$^+$ (**B**) T-cell proliferation (left) was measured by CFSE dilution. (**B**) CD4$^+$ results were not statistically significant. (**C**) IFNγ in the culture media were measured using human IFNγ ELISA kit. P-values by paired t-tests. *P<0.05. NS, not significant. (**D**) Immunoblotting showing HER2 levels in *NF1*$^+$ and *NF1*^{KO} MCF7 cells. (**E**) Indicated MCF7 cells were co-cultured with HER2-targeting CAR-T cells for 24 hours. The resulting cells were labeled by 7-AAD (7-Aminoactinomycin D) and BD Horizon™ V450-conjugated Annexin V to mark apoptotic cells before FACS. (**F**) Flow chart and quantification of apoptotic HER2-CAR-T cells. (**E, F**) P-values by paired t-test.

Model



Acknowledgement

This work was supported by CPRIT RP210027 - Baylor College of Medicine Comprehensive Cancer Training Program and DoD breast cancer program DAMD W81XWH-21-1-0634, the Cytometry and Cell Sorting Core at Baylor College of Medicine with funding from the CPRIT Core Facility Support Award (CPRIT-RP240432) and the NIH (CA125123, OD036336, and OD038251), and the assistance of Joel M. Sederstrom.